40. PV-Symposium 2025

Conference papers

https://doi.org/10.52825/pv-symposium.v2i.2649

Published: 27 Aug. 2025

The Increasing Importance of the Substructure for PV Modules Under High Mechanical Loads

Matthias Pander[1,2,*] and Bengt Jaeckel[1,2]

[1]Fraunhofer - Center for Silicon Photovoltaics CSP, 06120 Halle (Saale), Germany

[2]Fraunhofer Institute for Microstructure of Materials and Systems IMWS, 06120 Halle (Saale), Germany

*Correspondence: Matthias Pander, Matthias.pander@csp.fraunhofer.de

Abstract. With the introduction of new cell formats M10, M10R, and especially M12, PV modules have significantly increased in size. The availability of thin tempered glass (<2 mm) has led to a rise in glass-glass modules, which offer a high moisture barrier and minimize cell breakage by placing cells in the neutral axis. However, this increase in size also results in higher weight. To mitigate this, both glass thickness and frame height are being reduced, which brings the mechanical load-bearing capacity of glass and frames into focus. The mechanical stiffness of current frames (28 to 35mm height) is considerably lower than older frames (40mm and above), leading to greater flexibility and deformation under mechanical loads. As material thickness remains typically constant, the strength requirements for components increase. Increased deflection can cause contact between the PV module and substructure at loads significantly below 2,400 Pa (IEC 61215-2 minimum load). While this was not a major concern in the past, module manufacturers now actively exploit it for load approvals. Installers of small PV systems must carefully read installation manuals to understand permissible loads. The situation is even more critical for large systems that utilize bifaciality, as the entire load is transferred through the frame and clamps/screws. Finite element simulations and mechanical load tests demonstrate the importance of using the correct substructure for testing the mechanical load capacity of PV modules and highlight potential interactions. Various module sizes and substructure variants are simulated to compare deformation and stress results.

Keywords: PV Module, Mechanical Load, Finite Element Simulation, Glass Fracture Strength

1. Introduction

For a long time, crystalline solar modules were very robustly built in terms of glass and frame. The IEC standard loads of 5,400 Pa pressure and 2,400 Pa suction primarily posed a challenge regarding cell breakage [1]. Monocrystalline cells and thinner connectors have reduced the internal stresses in the cells, and the introduction of glass-glass modules positions the cell strings in the neutral axis of the module laminate, so that cell breakage can now occur only in exceptional cases due to pre-damage and handling. However, by optimizing weight and packing density, the glass and aluminium frame are now being pushed to their load limits. It is now very important to follow the exact configuration in the installation instructions for which the maximum load approval applies. This usually involves a four-point support system where screws or clamps are placed at fixed positions and typically prevent utilization of bifaciality. Especially for trackers in the inner positions (approximately 400 mm support distance), significantly lower load specifications arise. This contribution aims to show how high the load levels of current modules are and how little reserve is currently available. However, for challenging

environments such as floating PV, higher load levels exist, which require additional load reserves or modified support configurations.

For this investigation, we focus on current PV module sizes from major manufacturers (including Trina, Longi, Jinko, JASolar), which achieve relatively uniform module sizes depending on the cell format. The current external dimensions of the modules range between 1722 x 1134 mm² (residential) and 2384 x 1303 mm² (utility) according to the ITRPV [2]. Another focus is on glass-glass modules with a nominal glass thickness of 2 mm. For smaller module formats, modules with 1.6 mm glass are already available. For the specific investigations, current datasheet information for module layout, frame, and mounting will be used as the starting point (see Figure 1). The Longi module is an example for use in utility scale power plants. The dimensions result from the use of half-cut square M10 (182 x 91 mm²) cells. Larger cell formats like half-cut G12 (210 x 105 mm²) or rectangular cells (M10R, e.g. 182 x 105 mm²) lead to even larger module formats, which are examined in section 3.3. The Jinko module is an example of a residential module with an area of almost exactly 2m².

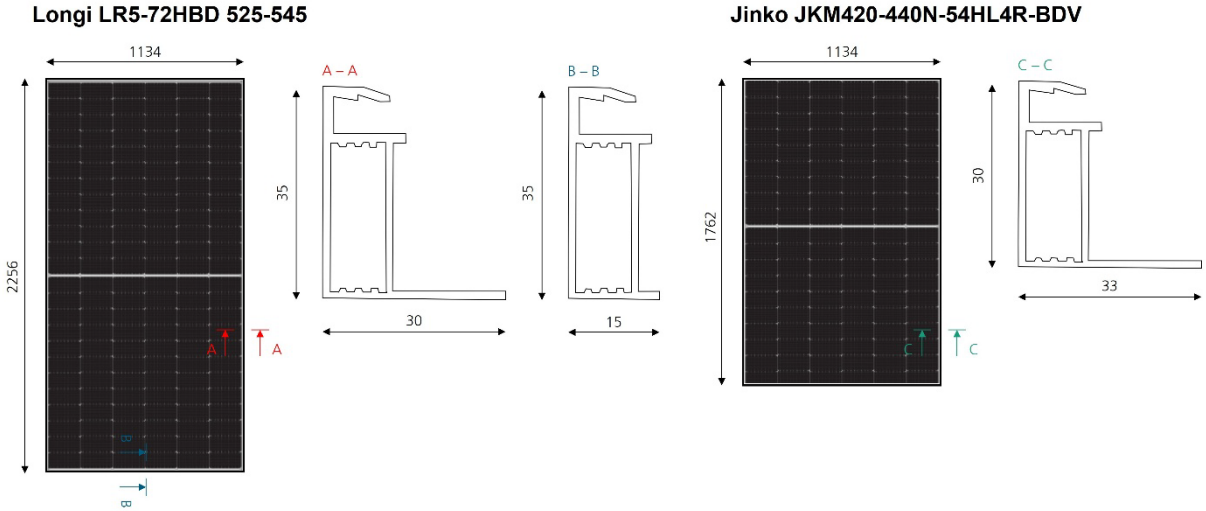

Figure 1. left) *datasheet information for Longi LR5-72HBD 525-545 [3] and* ***right)*** *Jinko JKM420-440N-54HL4R-BDV [4]*

2. Finite Element Simulation

2.1 Model setup

The load simulation is performed using a parameterized finite element model. In previous studies, a simplified model of thin-film modules and crystalline solar modules has already been developed ([5], [6], [7]). The geometry parameters include the specification of glass size, cell size and quantity, and the dimensioning of frame height, width and thickness to account for current and future module variants. Symmetry is utilized, such that only a quarter of the module is simulated. Contrary to previous simplifications with fixed support at the clamp, further elements of the substructure, such as cross beams or longitudinal supports, are now considered (see Figure 2). Cell connections can be neglected when using effective strength values for the cells like in [8]. The reference module laminate has a cell thickness of 160 µm, a thickness of the front encapsulation film of 400 µm, a thickness of the back encapsulation film of 400 µm, and a glass thickness of 2 mm each. The basic frame structure consists of a hollow chamber profile, as depicted in the drawings in Figure 1, and is parameterized to represent various sizes. The current frame heights range from 28 mm to 35 mm, with the default height of 30 mm used in this study. At the corners, the frame is firmly connected, which is a simplification as the connection is stronger than in reality. The laminate-frame connection represents a bonded contact by silicone rubber material. A significant difference from previous load simulations is

that the interaction of the module with the substructure (cross beam) is considered. For this purpose, contact elements with standard contact behaviour are used which lead to load transfer when contact is established.

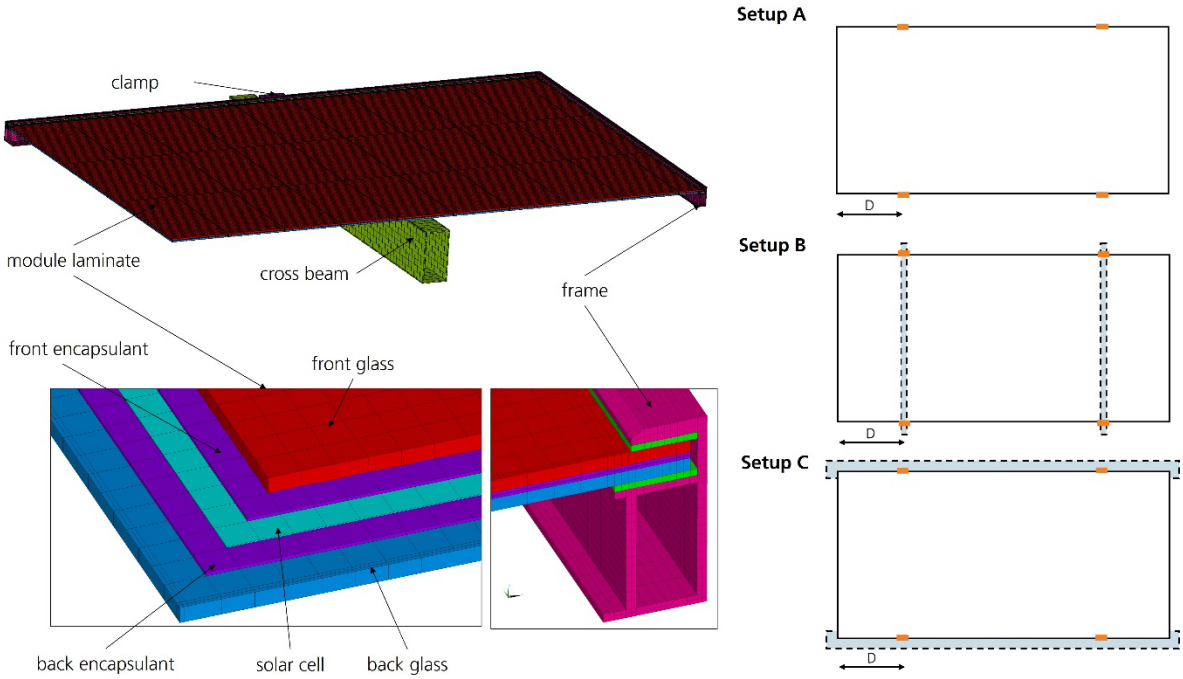

Figure 2. *Schematic structure of the finite element model with cross beam and overview of the investigated mounting setups*

The following support configurations are investigated (see Figure 2):

Clamping at the long module side without interaction with the support (Setup A): In this configuration the frame is only supported at the clamping position over the width of the clamp.

Clamping at the long module side with cross beam (Setup B): In this configuration a cross beam with a cross section of 40 mm width and 80 mm height with 2 mm wall thickness is used. The cross beam acts as additional support when the back side of the module comes into contact with it.

Clamping at the long module side with full support of the frame without cross beam (Setup C): This configuration is common for bifacial modules where the complete long side of the module is in contact with the bottom of the frame. Standard support depth is 15 mm in this investigation. The line support is rigid and will not deform in the simulation. The effects of possible deviations are briefly described in section 3.3.

The clamping position is also variable but is initially set at the specified average from the installation manual where D = L/5 for the 1762 x 1134 size and L/4 for the 2256 x 1134 size. It should be noted that the permitted deviations from this optimum position in the manuals are very small at ±50 mm. A clamp width of 50 mm is used, which is the minimum recommended size in the manufacturer manuals. For the load, the homogeneous test load is used according to the mechanical load profile of IEC 61215 MQT 16 [9]. The load is applied gradually to enable the analysis of specific load levels.

The deflection of the module at various positions is initially evaluated as a simple measurable parameter. The further evaluation of the results focuses on three key aspects. The stresses in the solar cells are expected to be low in the glass-glass configuration, but they are nevertheless analysed for comparison. For the breakage of the glass, the first principal stress

is analysed, which is the essential parameter for the brittle material. For the frame, the von Mises equivalent stress is the evaluation parameter to determine whether the load remains below the yield point.

The naming scheme 1762x1134_Setup_A_h30_2.0_2.0 is used for the brief description of the variants. It means 1762 mm length and 1134 mm width in the setup A with a frame height of 30 mm and a glass thickness of front and back glass of 2.0 mm respectively.

2.2 Material Data

For simulation of the materials literature data as well as internal measurements are used (Table 1). The encapsulant is modelled with visco-elastic behaviour therefore also the load rate is playing a role in the simulations. The aluminium material data is based on tensile tests on samples cut from the flange of a standard module frame. The corresponding curve is given in Figure 3 left. Based on the experience of Fraunhofer CSP, the known load limits for common aluminium frame material are between 210 and 262 MPa.

For classification purposes, the probability of failure needs to be estimated based on strength data of glass. The glass strength depends on various factors, in particular surface and edge defects. The quantity, size, position and orientation of these defects lead to a scattering of strength values. Therefore, there is a spread of fracture strength values. In addition, the size of the samples influences the strength value, which is referred to as the size effect. This is mentioned in DIN 1288-1, among others, according to which the strength in small test surfaces can be 140-270% higher than that of large test surfaces [10]. It also means that data generated by small ring-on-ring bending tests [11] are useful for comparison of glass batches but must be used with care and only under consideration of the size effect.

***Table 1**. overview of used material data*

Material and reference	Material model	Density [kg/m³]	Young's modulus [MPa]	Poisson ratio [-]
Glass [12]	Linear elastic	2500	70000	0.23
EVA [13]	Linear-viscoelastic	960	relaxation curve	0.4
Mono-crystalline silicon [14]	Anisotropic Linear elastic	2330	elasticity matrix 130024* (x-direction)	elasticity matrix 0.2785* (prxy)
Aluminium	Linear elastic	2700	67610	0.345
Aluminium (plastic)	Bilinear-elastic plastic	2700	67610 Yield strength 235.2 and 678.5 tangent modulus	0.345

*values for reference

For 2 mm module glass, strength data was measured with a specific large scale 4-point bending setup at the Fraunhofer CSP (bearing distance 1185 mm, load span: 880 mm). Results and details about the setup were presented at the glasstec conference in 2022 [15]. The description of the strength distribution is possible with the Weibull distribution as shown in Figure 3 right.

$$P_f = 1 - EXP\left(-\left(\frac{\sigma}{\sigma_\theta}\right)^m\right) \quad (1)$$

P_f – probability of failure

σ_θ – characteristic strength

m – Weibull modulus

σ – fracture stress

The specific result was σ_θ = 154.4 MPa, m = 10. It should be noted that the strength can vary depending on the manufacturer and production batch and there is currently no known systematic quality assurance. For “classic” heat strengthened glass with a thickness of 3.2 mm it can be assumed that the strength is at least as high or higher. Values of around 180 MPa were measured here. Thinner glass will have an even lower strength without special treatment. However, as there is currently no public data for 1.6 mm glass available, it is assumed for the purposes of this paper that the strength distribution is the same.

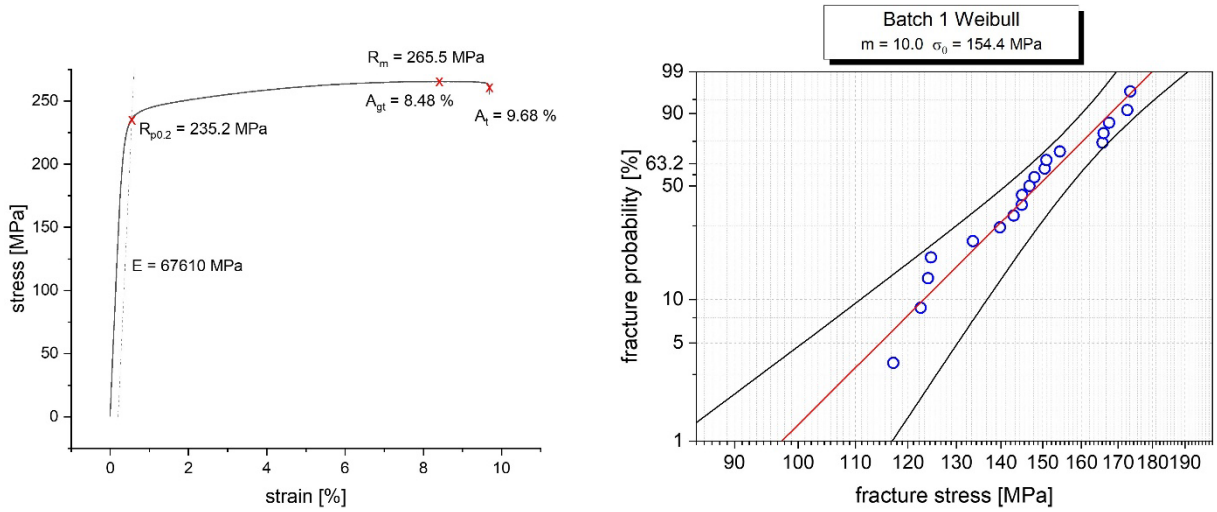

Figure 3. left) *tensile stress strain data for Aluminum frame material* ***right)*** *Weibull distribution for front glass strength test (2075 mm x 1024 mm x 2 mm glass)*

3. Results

3.1 Clamping at the long module side with and without cross beams

This section will show how the interaction with the cross beams contributes to the different load-bearing capacities. The maximum deformation for different small module format configurations is shown in Figure 4 left. It is clear from the deformation that interaction with the cross beams must take place as soon as the deformation exceeds the initial distance between back glass and base of the frame (~ 21.8 mm for the 30 mm). Contact with the cross beam already occurs between 1,400 and 1,800 Pa and occurs earlier for thinner glasses. The contact point is clearly visible from the change in the slope of the curves.

The maximum 1st principal stress of the cells is only of interest for the glass backsheet variant. Here, stresses are reached in some cells that can at least lead to occasional breakage (Figure 4 right). In the glass-glass variants, due to the position in the neutral axis, the stresses are, as expected, so low that cell breakage or crack propagation is very unlikely. This has also been observed in other variants and is therefore not discussed further.

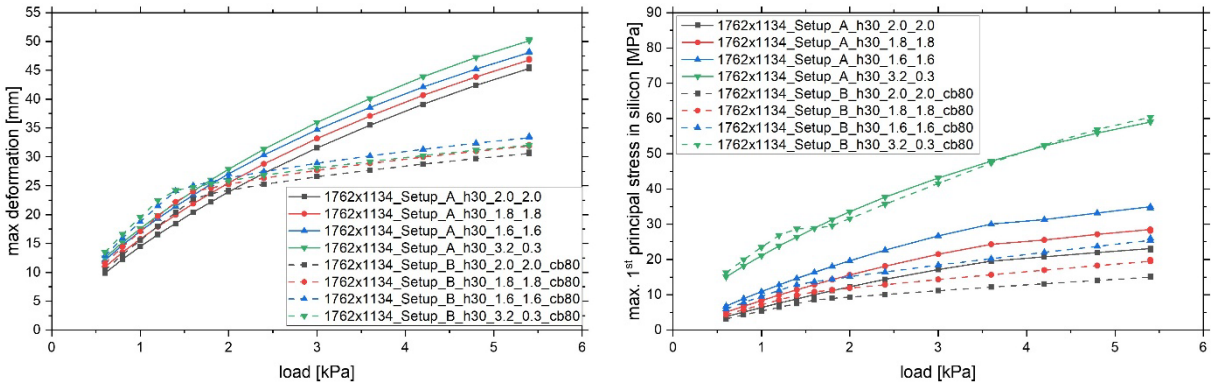

Figure 4. *Simulation results for four configurations of small format 1762 mm x 1134 mm with and without crossbeam* ***left)*** *max. deformation* ***right)*** *max. 1st principal stress in solar cell.*

In the following, the stress distribution in the glasses is reduced to the maximum stress value, which in some cases does not adequately describe the complexity of the load situation. Therefore, the contour plots are shown in Figure 5 for visualization purposes. On the one hand, the maximum is found in the front glass at the clamping positions, both in the front and rear glass with same order of magnitude. The support by cross beams causes a shift in the stresses and an additional tensile stress region is created via the cross beam. The backside of the front glass is relatively uncritical, but for the back glass there is a large tensile stress area on the bottom side, which is also changed in size when the support is present.

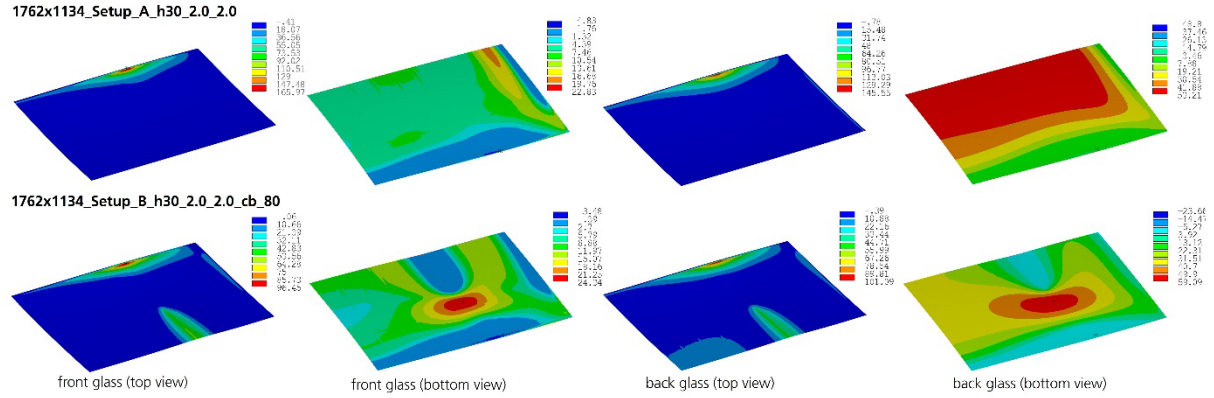

Figure 5. *Contour plot results of 1st principal stress for comparison of modules with and without crossbeam support, load 5.4 kPa. Note: color code changes for more clarity.*

Figure 6 shows the stresses in the glass. The support effect is clearly visible here. When contact between glass and cross beams is established, the increase in stress is significantly reduced and thus the stress is effectively reduced for the same load. The load is transferred more directly to the support structure. It should be noted that the stress in the 3.2 mm glass is significantly lower compared to 2x1.6 mm, whereby it must be assumed that the real strength of 1.6 mm glass is also lower. As previously noted, the stress on the top side of the front and back glass is similar, with an additional stress on the bottom side of the back glass. For classification purposes, the probability of failure may be estimated based on strength data of 2 mm glass given in section 2.2. A value of 114.6 MPa gives a fracture probability of 5 %. This is only a rough estimate because the size effect of fracture strength is neglected here but the basis is at least the test of full-size glass. For 2x2 mm with support the front glass reaches 96.5 MPa (P_f = 0.9 %) and the back glass 101.1 MPa (P_f = 1.4 %). The evaluation of results of the glass stress without support yield fracture probabilities of about 25 % at 3.6 kPa, which is consistent with approvals given by the manufacturers (Figure 7).

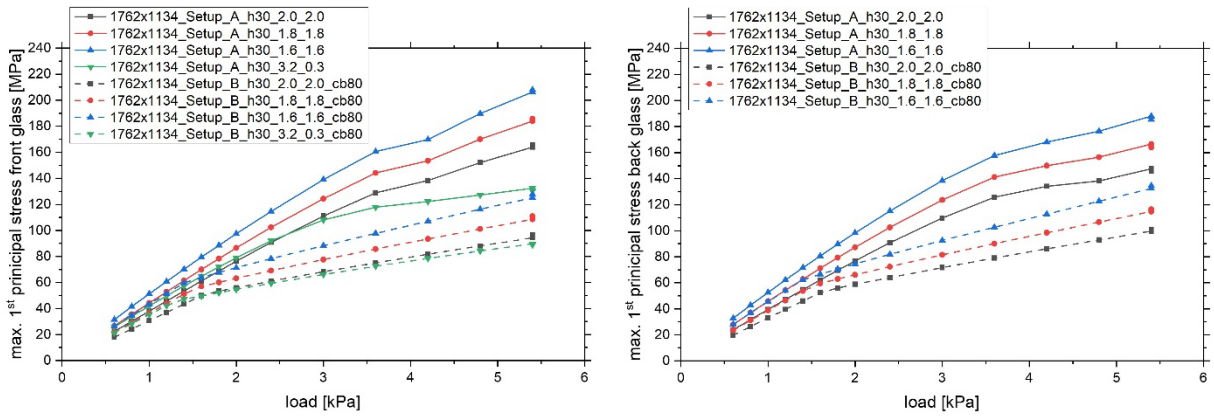

Figure 6. *Simulation results for four configurations of small format 1762 mm x 1134 mm with and without crossbeam* ***left)*** *max. 1st principal in front glass* ***right)*** *max. 1st principal stress in back glass.*

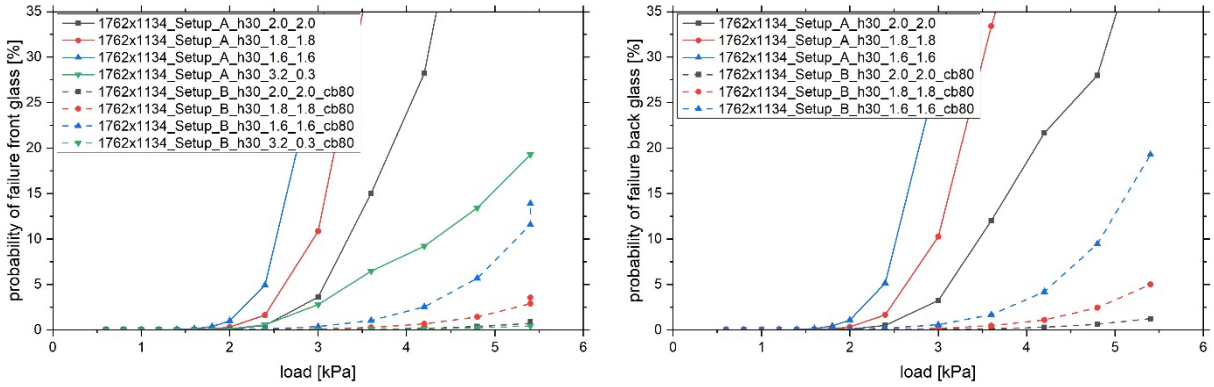

Figure 7. *Simulation results for four configurations of small format 1762 mm x 1134 mm with and without crossbeam* ***left)*** *estimated probability of failure in front glass* ***right)*** *estimated probability of failure in back glass.*

Figure 8 shows the results for the frame. Here too, contact with the cross beams leads to reduced stresses of the frame. Without the support, plastic deformation of the frame is likely in addition to the increased probability of the glass failure. The yield stress of aluminium frames based on internal measurements by Fraunhofer CSP and is indicated by the dashed lines in Figure 8.

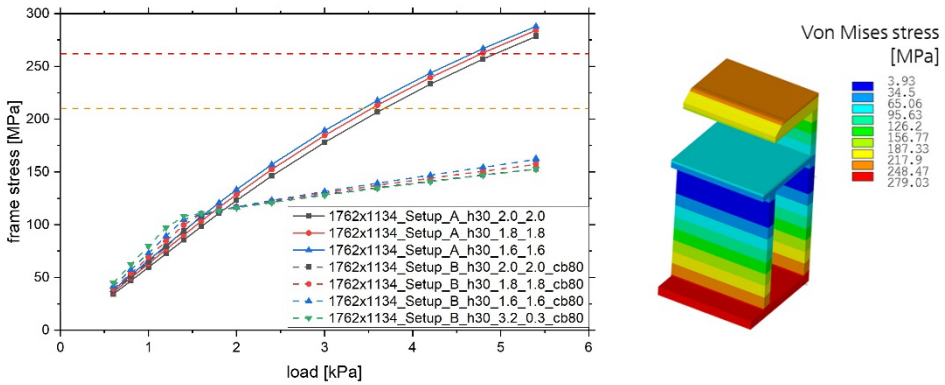

Figure 8. *Simulation results for four configurations of small format 1762 mm x 1134 mm with and without crossbeam* ***left)*** *von Mises stress in aluminium frame* ***right)*** *contour plot of the frame stress for 1762x1134_clamps_Setup_A_h30_2.0_2.0 at 5.4 kPa.*

3.2 Clamping at the long side with different cross beam stiffness

In the previous section the influence of the support by an almost rigid cross beam with 80 mm height was shown. In another study a more flexible cross beam with only 40 mm height is considered as well as a larger module format. For both module formats the clamping position D is ¼ of the module length. Note that this position results in 5 MPa higher stress in the glass compared to the previous simulations.

Comparing the maximum stress in the glass there is visible difference of 3.1 MPa (+2.9 %) for 1762x1134 and 2.7 MPa (+2.4 %) for 2256x1134 at the maximum load (Figure 9 left). Despite these changes seem to be small the stress level is in a range where fracture becomes more likely according to the strength parameters. The probability of failure increases from 3.5 to 4.5 % and 6.7 to 8.4 %. Regarding the stress in the frame there is also an increase, but it is below the yield strength of the frame (Figure 9 right).

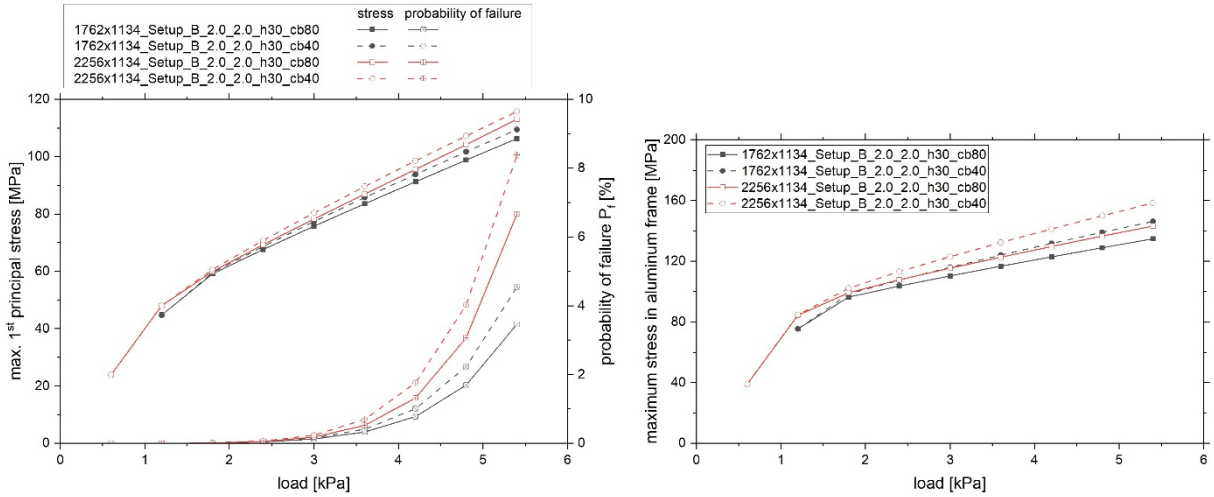

Figure 9. *Simulation results for Setup B with different cross beam height* ***left)*** *max. 1st principal stress in glass and probability of failure* ***right)****.*

These results are consistent with observations from laboratory tests (Figure 10). Despite approval up to 5.4 kPa, similar modules from different manufacturers did not pass the test in some cases. The fracture origin also corresponds to the maximum stress in the glass.

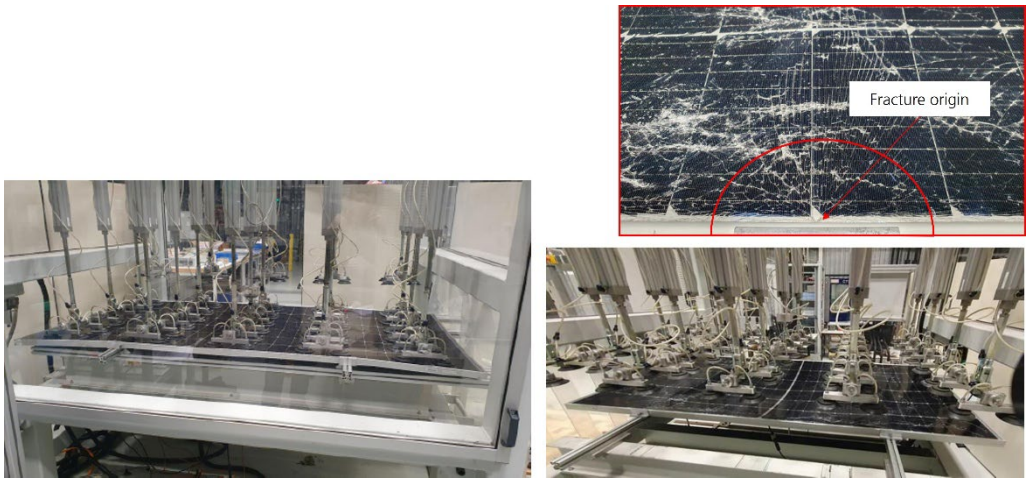

Figure 10. *Photos of mechanical load test of 2278 mm x 1134 mm modules with load of 5.4 kPa.*

The fact that larger modules such as 2384x1303 also exist initially results in a larger overhang (distance D increases) with the same clamping dimensions. This further increases the

stresses in the clamping area. Contact with the cross beams under compressive load is likely to occur even earlier and, in general, deviations from the optimum position will further increase the stress in the glass.

3.3 Line Support and large Modules

For the unsupported linear bearing, required for bifacial application, the frame loading becomes a critical factor. In this analysis, the plastic deformation of the Aluminium was incorporated using a bilinear plastic model with a yield strength of 235 MPa. Once the material's yield strength is reached, the deformation curves begin to diverge (Figure 11). Particularly with the large span of 1303 mm, a comparably low compressive load (2.4 kPa) results in first plastic deformation. For the smallest module size a load of 3.6 kPa is necessary for plastic deformation. This is consistent with the values provided in the installation manuals. An option that is especially available for the largest modules is an increased frame height of 35 mm that increases its stiffness. This is also visible in the results, but the effect is limited to support the short side of the module and shifts the plastic deformation to about 100 Pa higher loads. Regarding the stress in the glass, the increase in probability of failure and plastic deformation is happening at the same load level (Figure 12). Again, the maximum stress appears in the clamping region and is a result of the restriction of frame rotation by the clamp which is tried to visualize by the frame deformation plot in Figure 12.

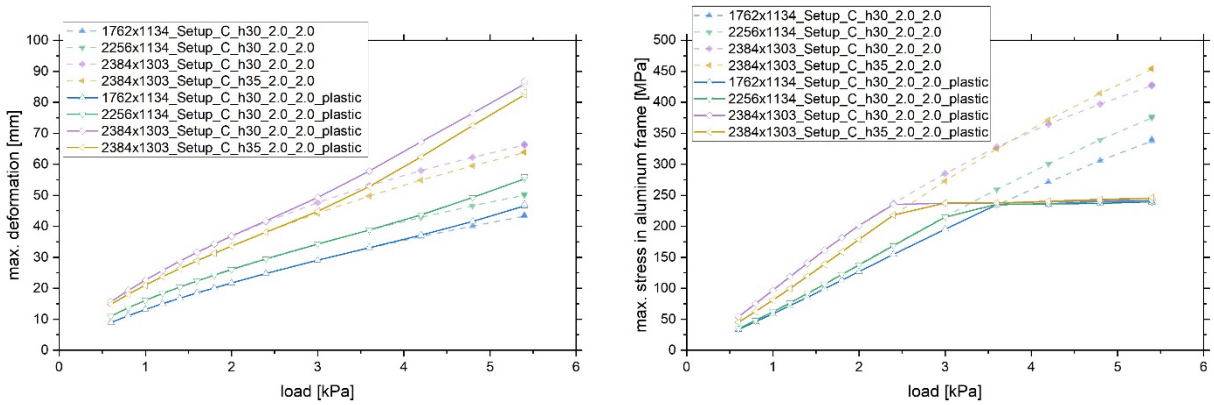

Figure 11. left) *max deformation of for setup C configurations* ***right)*** *max. stress in aluminium frame.*

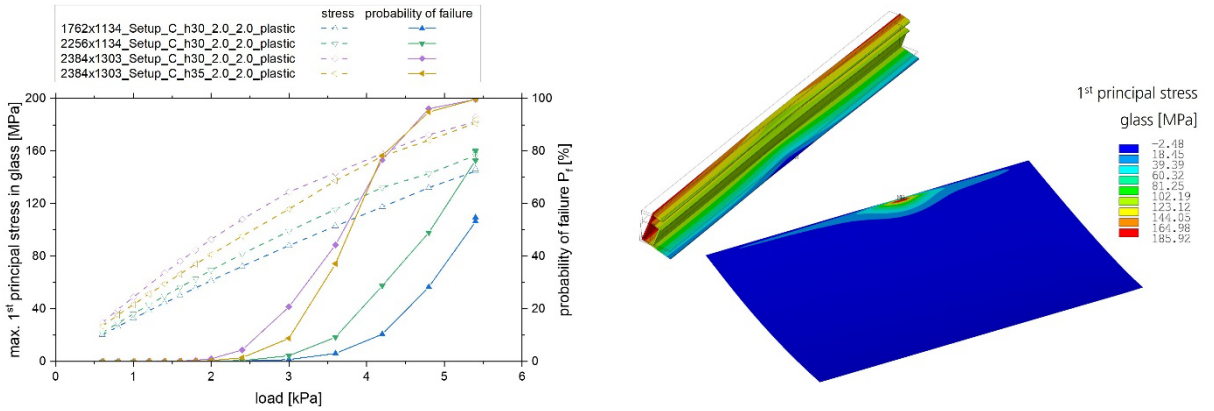

Figure 12. left) *max 1st principal stress in glass for setup C configurations* ***right)*** *contour plot of 1st principal stress in glass at 5.4 kPa for 2384x1303_Setup_C_h30_2.0_2.0 and corresponding frame deformation plot in the clamping region.*

Figure 13 shows the stress on the bottom of the back glass. While the maximum stress near the clamp on the front glass was not considerably affected, the plastic deformation of the frame leads to larger deformation at high loads and as consequence to increased stress on

the back glass. Considering that a large area of the glass is under tension a fracture of the back glass may be possible.

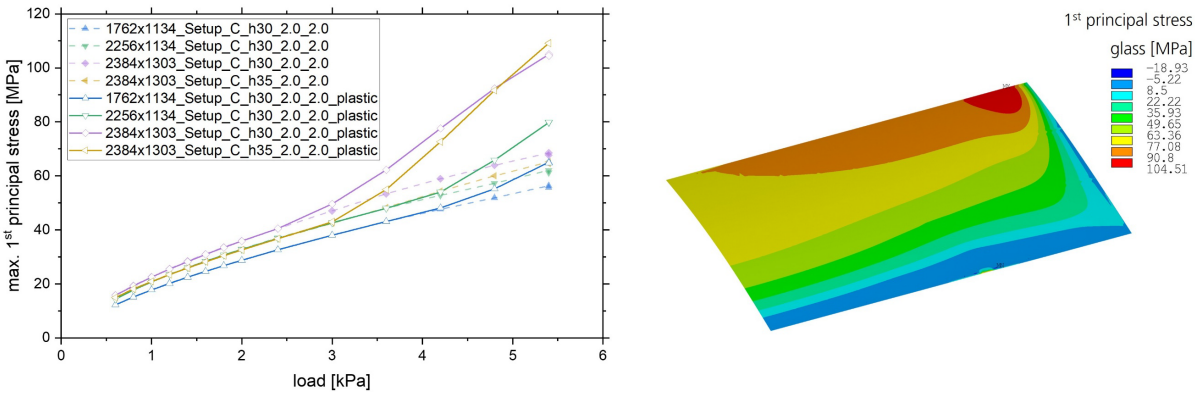

Figure 13. left) *max. 1st principal stress on bottom of back glass for setup C configurations* ***right)*** *contour plot of 1st principal stress on bottom side of back glass at 5.4 kPa for 2384x1303_Setup_C_h30_2.0_2.0.*

The last study will show that small changes can have very large effects on the overall system. Firstly, the support of the frame is reduced from 15 mm to 10 mm. This leads to a reduction in the clamping effect and the tension in the glass (Figure 14). However, the frame can also be fixed by screwing to the base of the frame. With this type of mounting, the frame can rotate with less restriction and as a result the previously high tensile stress in the front glass does not occur. The disadvantage of this change, however, is that it results in greater deflection and a higher load on the bottom of the back glass. Although the level of stress does not initially appear to be critical, taking into account the size effect and the large area under tension, an increased probability of breakage was determined on the rear side of the back glass.

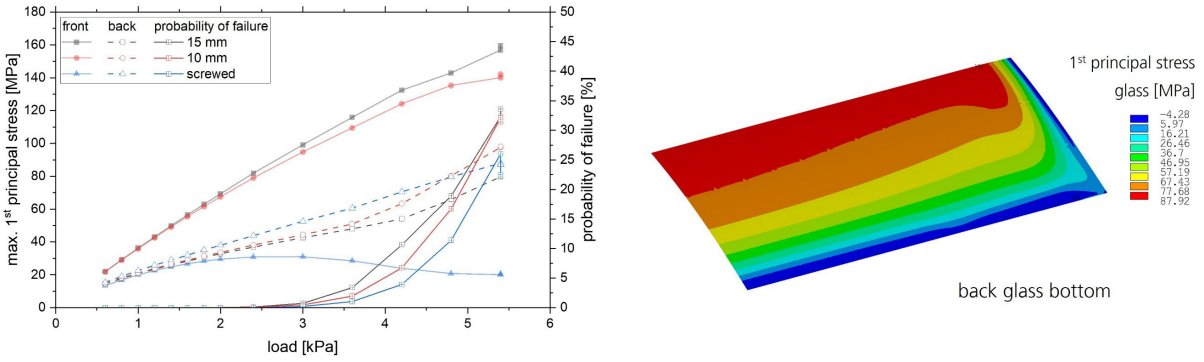

Figure 14. left) *Simulation result of max 1st principal stress in glass for two different support areas and screw mounting of 2256x1134_Setup_C_h30_2.0_2.0* ***right)*** *contour plot of 1st principal stress on bottom side of back glass at 5.4 kPa for screwed setup.*

A brief cross-comparison with laboratory observations also reveals very good agreement. On the one hand, modules could be tested in the line support configuration resulting in only the frame being plastically deformed at maximum load, but both glasses were still intact (Figure 15 left). On the other hand, there was a breakage of the back glass as predicted in the last example (Figure 15 right) while using screws on the bottom of the frame to mount the module onto the support structure.

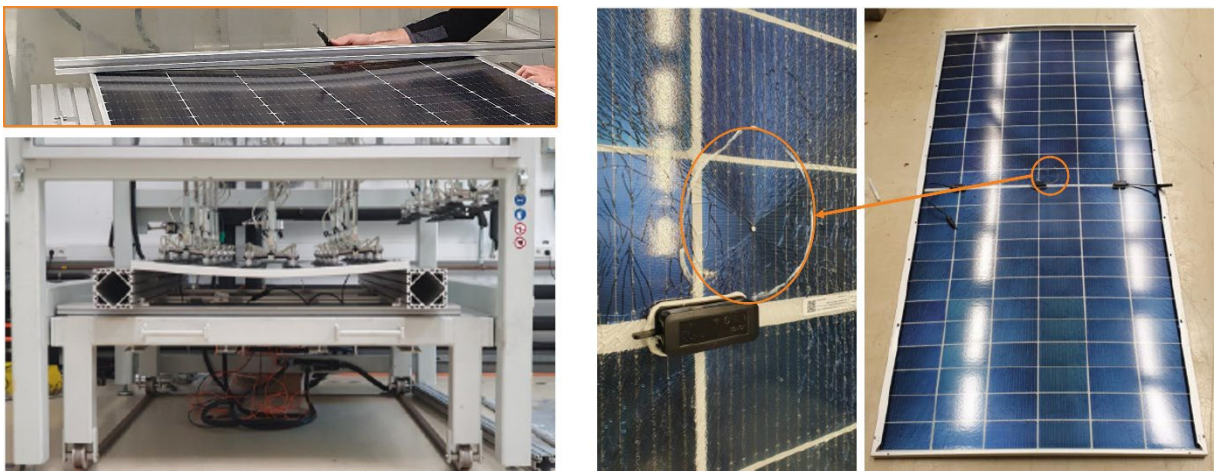

Figure 15. left) *2278x1134 module after 5700 Pa pressure load without failure using clamps, frame is plastically deformed and glass is still intact* ***right)*** *2384x1134 module with screwed mounting of the frame, glass fracture of the back glass at 3.6 kPa.*

4. Summary and conclusion

This paper demonstrates how significantly the load limits of current modules depend on the installation method. The high load ratings listed in data sheets are achievable only under very specific optimized mounting conditions. Several factors are crucial for proper installation like the clamp length and distance and even in optimal conditions as in current study the manufacturers work at the limits. Small deviation as they are unfortunately common in real installations (too small clamps, too close distance, support depth too small) lead to decrease load bearing capacity and thus to an increase in the probability of failure. Therefore, it is crucial to verify the information provided in the installation manuals and the associated boundary conditions. Validation of the specified test and design loads must be conducted by testing the combination of the module and the substructure together.

The mechanical load test (IEC 61215 MQT16) is in itself only a simplification of the real loads and it has already been shown in the literature that inhomogeneous loads can already use up the safety factor of 1.5 [16],[17]. The particularly high loads are achieved through contact with the cross beams of the substructure, which changes the mechanical system. It remains uncertain whether surface damage could occur from frequent impact-like contact with the support, particularly in cases of excessive flexibility caused by thinner glasses. Currently, contact already occurs at pressures ranging from 1.2 to 1.4 kPa, significantly lower than minimum type approval load of 2.4 kPa.

The main failure mechanism in the mechanical load test has changed for glass-glass modules. Instead of cell breakage, we now see glass breakage and plastic deformation of the frame as the dominant issues. This change creates a challenge because the regular testing scope, which typically involves only 1-2 modules, is too small. As a result, it is difficult to achieve statistical certainty about the design's performance based on such limited testing. For batch testing in the glass industry, at least 20-30 glass panes are tested to correctly describe the scattering [18].

Simulation models assist in deriving quality requirements for the components, guiding the choice of the combination of substructure and PV module, as well as estimating failure probabilities. The impact of variation in the mounting (clamp size and position) as mentioned before can easily be determined by a simulation model. Suitability of the frame material can be ensured relatively easy using standard tensile tests. An essential prerequisite is to determine and regularly check the strength distribution of the module glass to ensure the load-bearing capacity of the modules especially after successful certification.

Data availability statement

The raw data of the results shown in this study are available from the corresponding author, M. Pander, upon reasonable request. The specific data of the finite element model cannot be made accessible for reasons of confidentiality and intellectual property.

Author contributions

Conceptualization, methodology, writing – original draft preparation: Matthias Pander, writing—review and editing Bengt Jaeckel, Matthias Pander

Competing interests

The authors declare that they have no competing interests.

Funding

This work was financially supported by the European Union (EU-HORIZON Project 101136142 - BAMBOO) and the Federal Ministry of Economics and Climate Protection (BMWK) as part of the Green Solar Modules project (03EE1161A).

References

[1] M. Köntges et al, Performance and reliability of photovoltaic systems: Subtask 3.2: Review of failures of photovoltaic modules: IEA PVPS task 13: external final report IEA-PVPS", Sankt Ursen: International Energy Agency Photovoltaic Power Systems Programme, 2014. [Online]. Available: https://edocs.tib.eu/files/e01fb16/856979287.pdf
[2] International Technology Roadmap for Photovoltaic (ITRPV), 15th Edition, 2024
[3] Datasheet Longi Solar Longi LR5-72HBD-520-545M.pdf, 2024
[4] Datasheet Jinko Solar JKM420-440N-54HL4R-BDV-F1.2-EN-4.pdf, 2024
[5] M. Pander et al., "Digital Prototyping – Application of Numerical Methods in Module Development", 36th EU PVSEC, 2019, doi: 10.4229/EUPVSEC20192019-4BO.11.2
[6] S. Dietrich et al, "Mechanical Challenges of PV - Modules and its Embedded Cells - Experiment and Finite Element Analysis", doi: 10.4229/24thEUPVSEC2009-4AV.3.43
[7] S. Dietrich, et al., "Introducing a Reliability Concept Based on Probabilistic Material Data of Glass for PV Modules", 26th EU PVSEC, 2011, doi: 10.4229/26thEUPVSEC2011-4AV.1.7
[8] M. Sander et al, "Systematic investigation of cracks in encapsulated solar cells after mechanical loading", Solar Energy Materials and Solar Cells", 2012, doi: 10.1016/j.solmat.2012.12.031
[9] IEC 61215-2:2021, Terrestrial photovoltaic (PV) modules - Design qualification and type approval - Part 2: Test procedures, 2021
[10] DIN EN 1288-1, Glass in building - Determination of the bending strength of glass - Part 1: Fundamentals of testing glass; German version EN 1288-1:2000
[11] J. Markert et al, "Mechanical Stability of PV Modules: Analyses of the Influence of the Glass Quality", PV-Symposium Proc, vol. 1, Aug. 2024. doi: 10.52825/pv-symposium.v1i.1237
[12] DIN EN 572-1, Glas im Bauwesen – Basiserzeugnisse aus Kalk-Natronglas – Teil 1: Definitionen und allgemeine physikalische und mechanische Eigenschaften, 2004-09
[13] M. Pander et al, "Thermo-mechanical assessment of solar cell displacement with respect to the viscoelastic behaviour of the encapsulant", 12th. Int. Conf. on Thermal, Mechanical and Multiphysics Simulation and Experiments in Microelectronics and Microsystems, EuroSimE, 2011

[14] R. Hull, “Properties of crystalline silicon”, INSPEC, Institution of Electrical Engineers, 1999
[15] M. Pander et al, “Mechanical strength testing and evaluation of thin large-format solar glasses”, glasstec conference presentation, 2022
[16] S. Dietrich, “Evaluation of Non-Uniform Mechanical Loads on Solar Modules”, IEEE 39th Photovoltaic Specialists Conference (PVSC), Tampa, FL, USA, 2013, pp. 2998-3003, doi: 10.1109/PVSC.2013.6745093
[17] P. Romer et al, "Effect of inhomogeneous loads on the mechanics of PV modules“, Prog. Photovolt: Res. Appl., 2023, doi: 10.1002/pip.3738
[18] F. A. Veer et al, “The strength of annealed, heat-strengthened and fully tempered float glass”, Fatigue & Fracture of Engineering Materials & Structures, 2009, 32: 18-25. doi: 10.1111/j.1460-2695.2008.01308.x